Cancer Letters 380 (2016) 47–58

Contents lists available at ScienceDirect

Cancer Letters

journal homepage: www.elsevier.com/locate/canlet

Original Articles

NCAM- and FGF-2-mediated FGFR1 signaling in the tumor microenvironment of esophageal cancer regulates the survival and migration of tumor-associated macrophages and cancer cells

Nobuhisa Takase [a,b], Yu-ichiro Koma [a], Naoki Urakawa [a,b], Mari Nishio [a], Noriaki Arai [a], Hiroaki Akiyama [a], Manabu Shigeoka [a], Yoshihiro Kakeji [b], Hiroshi Yokozaki [a,*]

[a] Division of Pathology, Department of Pathology, Kobe University Graduate School of Medicine, 7-5-1 Kusunoki-cho, Chuo-ku, Kobe 650-0017, Japan
[b] Division of Gastro-intestinal Surgery, Department of Surgery, Kobe University Graduate School of Medicine, 7-5-1 Kusunoki-cho, Chuo-ku, Kobe 650-0017, Japan

ARTICLE INFO

Article history:
Received 12 February 2016
Received in revised form 1 June 2016
Accepted 9 June 2016

Keywords:
NCAM
FGF-2
FGFR1
Esophageal cancer
Macrophage
Tumor microenvironment

ABSTRACT

Tumor-associated macrophages (TAMs) have important roles in the angiogenesis and tumor immunosuppression of various cancers, including esophageal squamous cell carcinomas (ESCCs). To elucidate the roles of TAMs in ESCCs, we compared the gene expression profiles between human peripheral blood monocyte-derived macrophage-like cells (Macrophage_Ls) and Macrophage_Ls stimulated with conditioned medium of the TE series human ESCC cell line (TECM) (TAM_Ls) using cDNA microarray analysis. Among the highly expressed genes in TAM_Ls, we focused on *neural cell adhesion molecule* (*NCAM*). NCAM knockdown in TAM_Ls revealed a significant decrease of migration and survival via a suppression of PI3K-Akt and fibroblast growth factor receptor 1 (FGFR1) signaling. Stimulation by TECM up-regulated the level of FGFR1 in Macrophage_Ls. Recombinant human fibroblast growth factor-2 (rhFGF-2) promoted the migration and survival of TAM_Ls and TE-cells through FGFR1 signaling. Our immunohistochemical analysis of 70 surgically resected ESCC samples revealed that the up-regulated FGF-2 in stromal cells, including macrophages, was associated with more aggressive phenotypes and a high number of infiltrating M2 macrophages. These findings may indicate a novel role of NCAM- and FGF-2-mediated FGFR1 signaling in the tumor microenvironment of ESCCs.

Introduction

The interaction between cancer cells and stromal cells produces a cancer-specific microenvironment for tumor progression [1]. Macrophages, one of the most important components of a tumor microenvironment, are divided into two phenotypes from an oncologic viewpoint: a tumor-suppressive (M1) phenotype and a tumor-supportive (M2) phenotype [2]. Tumor-associated macrophages (TAMs) polarize mainly into the M2 phenotype depending on microenvironmental factors [3,4]. M2 macrophages generally exhibit an interleukin (IL)-10^{high}, IL-12^{low} phenotype and demonstrate high expression of CD163 (a hemoglobin scavenger receptor) and CD204 (a class A macrophage scavenger receptor) [5,6]. Infiltrations of TAMs with the M2 phenotype correlate with poor prognosis in patients with various types of tumor [7–11].

Esophageal cancer is the sixth leading cause of cancer-related death and the eighth most common cancer worldwide. An estimated 455,800 new esophageal cancer cases and 400,200 deaths were recorded in 2012 worldwide [12]. Recent epidemiological studies reported that the number of esophageal adenocarcinomas has tended to increase in not only Western countries but also in Asian countries. However, squamous cell carcinoma of the esophagus (ESCC) still accounts for most of the esophageal carcinomas in the Asian countries, including Japan. Various factors, *e.g.*, alcohol and smoking, are considered to present a risk of ESCC development [13,14].

We reported that the number of infiltrating CD204^{+} macrophages in ESCC tissues exhibits a significant correlation with

Abbreviations: Ct, threshold cycle; Cyr61, cysteine-rich angiogenic inducer 61; DFS, disease free survival; DMEM, Dulbecco's Modified Eagle's Medium; ESCC, esophageal squamous cell carcinoma; FGF-2, fibroblast growth factor-2; FGFR1, fibroblast growth factor receptor 1; GDF15, growth differentiation factor 15; IL, interleukin; Macrophage_L_THP-1, TPA-treated THP-1 macrophage-like cell; Macrophage_L, PBMo-derived macrophage-like cell; M-CSF, macrophage-colony stimulating factor; MMP, matrix metalloprotease; NC, negative control; NCAM, neural cell adhesion molecule; OS, overall survival; PBMC, peripheral blood mononuclear cell; PBMo, peripheral blood monocyte; rhFGF-2, recombinant human FGF-2; TAM, tumor-associated macrophage; TAM_L, Macrophage_L stimulated with TECM; TAM_L_TE-9, Macrophage_L stimulated with TE-9CM; TAM_L_THP-1, Macrophage_L_THP-1 stimulated with TECM; TAM_L_THP-1_TE-9, Macrophage_L_THP-1 stimulated with TE-9CM; TECM, conditioned medium of the TE series ESCC cell line; THP-1, a human acute monocytic leukemia cell line; TPA, 12-*O*-tetradecanoylphorbol-13-acetate; VEGFA, vascular endothelial growth factor A.

* Corresponding author. Tel.: +81 78 382 5460; fax: +81 78 382 5479.
E-mail address: hyoko@med.kobe-u.ac.jp (H. Yokozaki).

http://dx.doi.org/10.1016/j.canlet.2016.06.009

clinicopathological factors and prognosis [10]. *In vitro* studies demonstrated that bone marrow-derived peripheral blood monocyte (PBMo)-derived macrophage-like cells (Macrophage_Ls) stimulated with conditioned media of ESCC cells (TECM) had significantly more enhanced M2-like genes than Macrophage_Ls, such as *IL-10*, *CD163*, *CD204*, *VEGFA*, *MMP2* and *MMP9* [15]. We also analyzed the up-regulated genes, including *cysteine-rich angiogenic inducer 61* (*Cyr61*) and *growth differentiation factor 15* (*GDF15*), using a cDNA microarray between Macrophage_Ls treated with and without TECM. The up-regulation of Cyr61 and GDF15 exhibited a significant positive correlation with infiltrating $CD204^+$ TAMs in human ESCC samples [15,16]. In the present study, among the highly expressed genes in Macrophage_Ls stimulated with TECM (TAM_Ls), we focused on *neural cell adhesion molecule* (*NCAM*).

NCAM is one of the immunoglobulin superfamily molecules isolated from chicken nerve retina cells [17–19]. NCAM has three major isoforms created by alternative splicing, and the extracellular part is comprised of five Ig modules and two fibronectin type III homology modules. NCAM is associated with neurite outgrowth and intracellular adhesion through homophilic and heterophilic interactions in the nervous system [20]. NCAM expression has been reported not only in nerve cells but also in various non-neural cell types, including monocytes [21]. NCAM is also involved in the progression of various types of cancer [22–25]. However, the significance of NCAM expression in TAMs has not been established, and here we investigated a potential role of NCAM expressed in TAMs in the ESCC microenvironment.

Materials and methods

Cell cultures and reagents

Three ESCC cell lines (TE-8, TE-9 and TE-15) were obtained from the RIKEN BioResource Center (Tsukuba, Japan). The individuality of the TE series ESCC cell lines was confirmed by a short tandem repeat analysis at RIKEN and at the Cell Resource Center for Biomedical Research, Institute of Development, Aging and Cancer, Tohoku University (Sendai, Japan). Human peripheral blood mononuclear cells (PBMCs) were obtained from healthy volunteer donors who provided written informed consent. We purified $CD14^+$ PBMos from the PBMCs by positive selection using an autoMACS Pro Separator (Miltenyi Biotec, Bergisch Gladbach, Germany).

The PBMos were treated with macrophage-colony stimulating factor (M-CSF, 25 ng/mL; R&D Systems, Minneapolis, MN) for 6 d to induce Macrophage_Ls and then exposed to the conditioned media of the TE series ESCC cell lines (TECMs) for 2 d to induce TAM_Ls as described [15]. All cells were mycoplasma negative as demonstrated by a Venor® GeM Classic Mycoplasma Detection kit (Minerva Biolabs, Berlin, Germany). The following selective inhibitors and recombinant protein were used: PI3K inhibitor (LY294002, 20 μM; Cell Signaling Technology, Beverly, MA); FGFR1 inhibitor (SU5402, 50 μM; Santa Cruz Biotechnology, Dallas, TX); human recombinant basic fibroblast growth factor (rhFGF-2, 5–20 ng/mL; R&D Systems).

Tissue samples

A total of 70 human ESCC tissue samples were examined in our study as described [10]. Informed consent for the use of the tissue samples was obtained from all patients, and the study was approved by the Kobe University Institutional Review Board. We analyzed histological and clinicopathological information using the Japanese Classification of Esophageal Cancer proposed by the Japan Esophageal Society and the TNM classification of the Union for International Cancer Control [26,27].

Immunohistochemistry

Antigen retrieval of 10% formalin-fixed and paraffin-embedded tissues was heat-induced in citrate buffer, pH 6.0. Immunohistochemistry was performed using EnVision Dual Link System-HRP, 3,3′-diaminobenzidine (Dako Cytomation, Glostrup, Denmark). The primary antibodies are listed in Supplementary Table S1. The FGF-2 immunoreactivity of the cancer nests and stroma was assessed separately. We evaluated the immunohistochemical staining intensity of FGF-2 in the cancer nests as qualitative scores: 0 (negative), 1 (weak), 2 (intermediate) and 3 (strong). We assessed the proportion of immune-positive stromal cells in the stroma by counting the number of these cells per high-power field as low (<30) and high (≥30) using the corresponding normal squamous epithelia as a positive control. The immunoreactivity of the cancer nests was considered high with a score of 2 or 3. We also determined the correlations between the expression of FGF-2 and clinicopathological parameters and the infiltrating macrophage phenotypes.

Immunofluorescence

Cultured cells were fixed with methanol (purity > 99.8%; Wako, Osaka, Japan). The primary and secondary antibodies are listed in Supplementary Table S1. Nuclei and F-actin were stained with DAPI (Wako) and phalloidin (P1951, Sigma-Aldrich, St. Louis, MO), respectively. These samples were observed under a laser-scanning microscope (LSM700, Carl Zeiss, Oberkochen, Germany) and analyzed using ZEN 2009 software (Carl Zeiss).

Reverse transcription-polymerase chain reaction (RT-PCR) and quantitative RT-PCR

We extracted total RNA from cultured cells using the RNeasy Mini Kit (Qiagen, Hilden, Germany). RT-PCR amplifications of *NCAM* and the control gene *GAPDH* were performed. We conducted the quantitative RT-PCR amplifications of *NCAM* and the control gene *GAPDH* using the ABI StepOne Real-time PCR system (Applied Biosystems, Foster City, CA). The primers listed in Supplementary Table S2 were designed as described [28,29].

Knockdown of NCAM by small interfering RNA (siRNA) and human phosphoprotein array

First, 1×10^6 Macrophage_Ls were transfected at 20 nM concentrations for 6 h with siRNA for *NCAM* (Sigma) or negative control (NC, S1C-001, Sigma) using Lipofectamine RNAiMAX (Invitrogen, Carlsbad, CA). The sequences of the siRNA targeting *NCAM* are as follows: *sense*, 5′-GAGGUAUUUGCCUAUCCCAtt-3′; *antisense*, 5′-UGGGAUAGGCAAAUACCUCtt-3′. Transfected cells were then exposed to TECM for 2 d to induce TAM_Ls and cultured for 24 h in serum-free Dulbecco's Modified Eagle's Medium (DMEM, Wako). The cell lysates were collected and applied to a Proteome Profiler Human Phosphokinase Array Kit (R&D Systems).

Enzyme-linked immunosorbent assay (ELISA)

Here, 5×10^6 TE cells were seeded on 100-mm dishes filled with DMEM supplemented with 10% human AB serum (Lonza, Walkersville, MD). Then, 1×10^6 Macrophage_Ls and TAM_Ls were incubated on six-well plates filled with DMEM supplemented with 10% human AB serum. After 2 d, the cells were collected and applied to a Quantikine ELISA Human FGF basic immunoassay (R&D Systems). We determined the optical density using a Microplate Reader Infinite 200 PRO (Tecan, Männedorf, Switzerland).

Western blotting

Cells were lysed in a cell lysis buffer (50 mM Tris–HCl pH 7.5, 125 mM NaCl, 0.1% Triton X-100 and 5 mM EDTA) or NP40 cell lysis buffer (Thermo Fisher Scientific, Waltham, MA). The resulting lysates were separated on 5 to 20% sodium dodecyl sulfate polyacrylamide gels and blotted with primary antibodies. The primary and secondary antibodies are listed in Supplementary Table S1. The blots were then probed with ImmunoStar Reagents (Wako).

Transwell migration assay and cell survival assay

Transwell migration assay

1×10^5 cells were detached with Accutase (Innovative Cell Technologies, San Diego, CA) or trypsin-EDTA (Thermo Fisher). The cells were then seeded on Transwell cell culture inserts (8-μm pore size filter, BD Falcon, Lincoln Park, NY) filled with serum-free DMEM for 24 h. The cell inserts were then set on the 24-well plates filled with DMEM supplemented with 1% human AB serum. After a period of 24 h, migrated cells on the underside of the membrane were stained with Diff-Quik (Sysmex, Kobe, Japan) and counted.

Cell survival assay

1×10^4 detached cells were seeded on 96-well plates (BD Falcon) filled with serum-free DMEM. After 24 h, we applied CellTiter 96 AQueous One Solution Reagent (Promega, Madison, WI). We determined the optical density of each well using the microplate reader.

Statistical analysis

We used χ^2-tests to analyze the relationships between clinicopathological factors and the immunohistochemical results. The statistical significance of differences in the *in vitro* assay results was evaluated by two-sided Student's *t*-test. Significance was set at a p-value < 0.05. The statistical analyses were performed with SPSS Statistics ver. 22 (IBM, Chicago, IL).

Results

NCAM expression in Macrophage_Ls is up-regulated by conditioned media of ESCC cell lines

We first confirmed the induction of NCAM in TAM_Ls. NCAM mRNA and protein expression was significantly induced by TECM (TE-8, TE-9 and TE-15) compared with the Macrophage_Ls (Fig. 1A–C). The expression of NCAM in the TAM_Ls was confirmed by the molecular weight 180 kDa (Fig. 1C). As the NCAM induction was most effective by TE-9CM, we focused on the Macrophage_Ls stimulated with TE-9CM (TAM_L_TE-9). The up-regulated NCAM was identified mainly in the cell membrane of TAM_L_TE-9 (Fig. 1D).

In contrast, the NCAM induction in M2 macrophages was not produced by the stimulation of IL-4 and IL-13 (Suppl. Fig. S1). We previously demonstrated that TECM induced the M2 phenotype in the 12-*O*-tetradecanoylphorbol 13-acetate (TPA)-treated human acute monocytic leukemia cell line (THP-1) macrophage-like cells (Macrophage_Ls_THP-1) [10]. In the present study, exposure to TECM significantly induced NCAM expression in Macrophage_Ls_THP-1 (Suppl. Fig. S2). Morphologically, a portion of the lamellipodia was co-localized with F-actin (phalloidin) and NCAM in the TAM_Ls_TE-9, implying that NCAM was involved in the migration of TAM_Ls (Fig. 1E).

NCAM is involved in TAM_L migration and survival through PI3K-Akt signaling

We then assessed the migration and survival of TAM_Ls. Exposure to TE-9CM significantly promoted the migration and survival of Macrophage_Ls (Fig. 2A). We next examined the role of NCAM in TAM_L_TE-9 by using siRNA. NCAM silencing was confirmed by RT-PCR, quantitative RT-PCR and western blotting (Suppl. Fig. S3). NCAM silencing resulted in significant decreases in the migration and survival of TAM_Ls_TE-9 (Fig. 2B).

Next, we conducted a phospho-kinase antibody array to assess the changing levels of phosphorylated proteins by NCAM knockdown. Interestingly, the silencing of NCAM in TAM_Ls_TE-9 suppressed PI3K-Akt (Thr308) and p70 S6K (Thr421/Ser424), namely PI3K-Akt signaling (Fig. 2C). Moreover, exposure to TECM (TE-8, TE-9 and TE-15) activated PI3K-Akt signaling in Macrophage_Ls (Fig. 2D). In addition, LY294002 (20 μM) significantly inhibited the migration and survival of TAM_Ls_TE-9 (Fig. 2E).

NCAM- and FGF-2-mediated FGFR1 signaling regulated the expression of phosphorylated FGFR1 in TAM_Ls

The interaction between NCAM- and fibroblast growth factor-2 (FGF-2)-mediated fibroblast growth factor receptor 1 (FGFR1) signaling is known to induce a specific cellular response in HeLa cells [30]. However, their expressions and interactions in the ESCC microenvironment, including macrophages, are not clearly understood. In the FGFR family, FGFR1 is expressed on human monocytes [31]. We thus investigated the functional role of FGFR1 signaling in TAM_Ls. Our immunofluorescence protocol demonstrated that NCAM was co-localized with FGFR1 at the cell membrane in TAM_L_TE-9 (Fig. 3A). Interestingly, NCAM silencing suppressed FGFR1 and its phosphorylation in TAM_Ls_TE-9 (Fig. 3B). Up-regulation of FGFR1 expression was induced in all types of TAM_Ls, and FGFR1 phosphorylation was also observed in the TAM_Ls (TE-9 and TE-15) (Fig. 3C).

We analyzed the secretion of FGF-2 from ESCC cell lines and TAM_Ls by ELISA. The secreted FGF-2 levels in TE-8, TE-9 and TE-15 were 20.58 ± 2.38 pg/mL, 12.74 ± 2.67 pg/mL and 0.98 ± 0.35 pg/mL, respectively. In contrast, FGF-2 secreted by TAM_Ls was not detected (Fig. 3D).

We then investigated the effect of FGF-2 on TAM_Ls. Interestingly, rhFGF-2 treatment resulted in phosphorylation of FGFR1 and the downstream signaling, such as PI3K-Akt and MEK1/2-Erk1/2. The phosphorylation level of the downstream signaling was maintained for up to 1 h in TAM_Ls_TE-9 (Fig. 3E). Pretreatment with SU5402 significantly inhibited the phosphorylation of FGFR1, Akt and Erk1/2 in TAM_Ls_TE-9 (Fig. 3E). In addition, TAM_Ls_TE-9 significantly promoted migration and survival by FGF-2, which was inhibited by SU5402 (Fig. 3F).

FGF-2-mediated FGFR1 signaling is involved in the migration and survival of ESCC cells

We next investigated the effect of FGF-2/FGFR1 signaling on ESCC cell lines. The expression of FGFR1 was detected in TE-8, TE-9 and TE-15 (Fig. 4A). Treatment with rhFGF-2 activated MEK1/2-Erk1/2 signaling in TE-9. Pretreatment with SU5402 significantly inhibited MEK1/2-Erk1/2 phosphorylation in TE-9 (Fig. 4B). FGF-2 significantly promoted the migration and survival of TE-9, which were inhibited by SU5402 (Fig. 4C).

Up-regulated FGF-2 in stromal cells, including macrophages, is associated with more aggressive phenotypes and an increased number of infiltrating M2 macrophages

FGF-2 overexpression has been reported in esophageal cancer, and this overexpression may lead to poor prognosis [32]. In contrast, Sugiura et al. reported a negative correlation between FGF-2 expression and clinical prognosis limited to ESCC [33]. We thus investigated the relationships between the expression levels of FGF-2 and clinicopathological parameters including M2 macrophage markers in ESCCs.

We first confirmed the expression of FGF-2 by demonstrating immunofluorescence mainly in the cytoplasm and nucleus of $CD204^+$ TAM_Ls_TE-9 (Fig. 4D). Interestingly, the double immunofluorescence analysis demonstrated that the FGF-2 was expressed not only in cancer cells but also in cancer stromal cells (including $CD204^+$ TAMs) in human ESCC tissues (Fig. 4E).

We next analyzed 70 ESCC tissue samples by immunohistochemistry to investigate whether FGF-2 expression levels were associated with clinicopathological background factors of ESCC patients. We evaluated FGF-2 expression levels in these tissues compared with the corresponding nonneoplastic squamous epithelium (Fig. 4F). We divided the site of localization of FGF-2 expression into three parts as follows: cancer stroma, cancer nests, and both cancer nests and stroma. These three parts were further categorized as low- and high-intensity groups (Fig. 4F). The high-intensity group in the cancer stroma exhibited significant positive correlations with the depth of invasion, blood vessel invasion, stage, and high numbers of infiltrating CD163-positive and CD204-positive macrophages (Table 1). The high-intensity group in the cancer nests had no significant associations with any of the clinical background factors (Table 1).

We next performed a prognostic study of 69 of the 70 ESCC patients (excluding the single patient who was lost to follow-up). A cumulative Kaplan–Meier analysis revealed that the patients who showed high-intensity group of FGF-2 in cancer stroma tended to have a shorter disease-free survival and overall survival (Suppl. Fig. S4).

Discussion

The results of the present study confirmed that NCAM expression was induced in TECM-induced Macrophage_Ls. The up-regulated

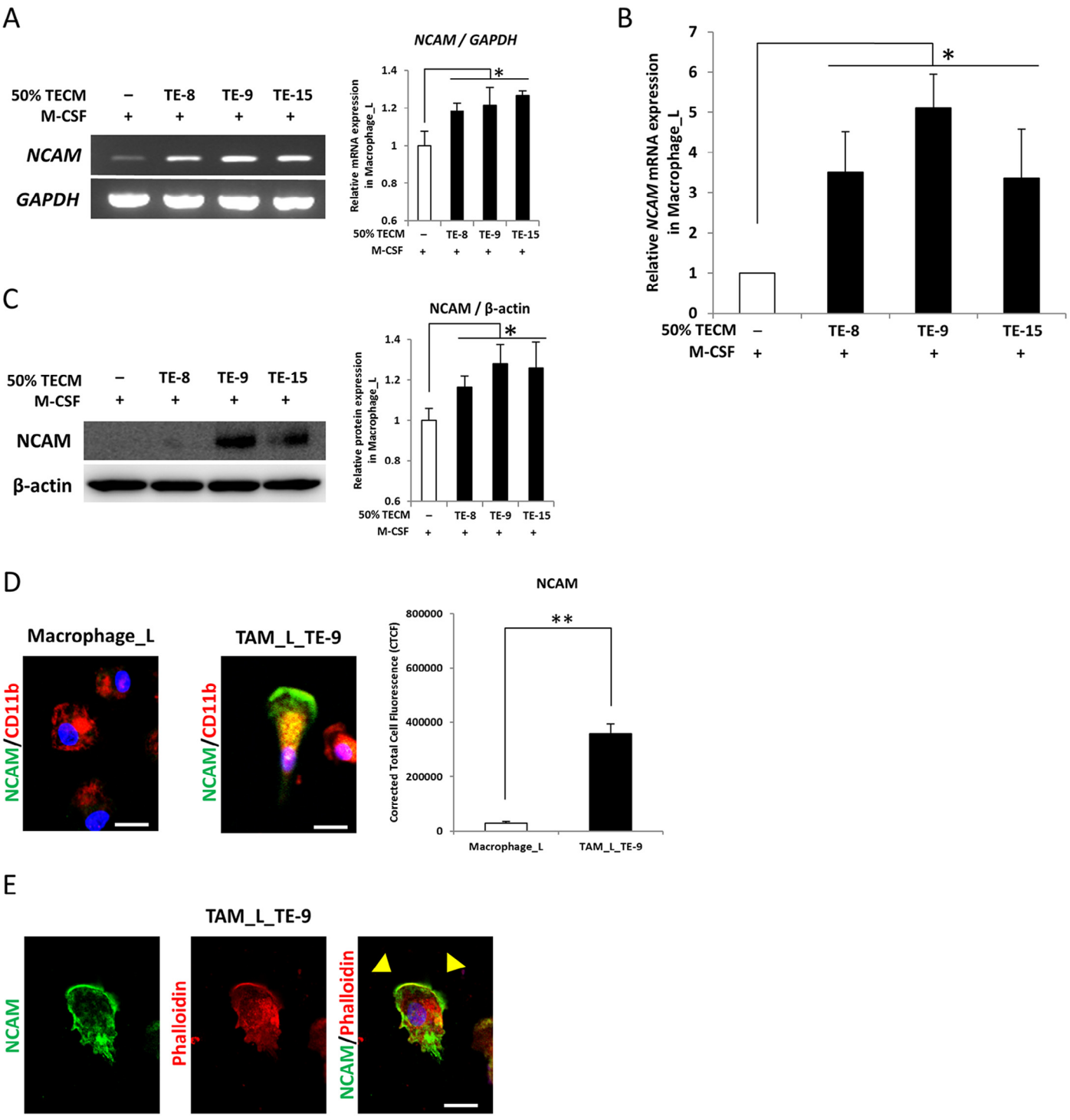

Fig. 1. Induction of NCAM in peripheral blood monocyte (PBMo)-derived macrophages stimulated with conditioned medium of a TE series ESCC cell line (TECM). PBMos were treated with 25 ng/mL recombinant human M-CSF for 6 d to induce Macrophage_L and then exposed to the TECM (TE-8, TE-9 and TE-15) for 2 d to induce TAM_Ls. (A) *NCAM* mRNA induction in the TAM_Ls was confirmed by RT-PCR (*left panel*). The results were normalized to *GAPDH* as a control, and densitometric analysis of bands was performed with ImageJ (National Institutes of Health, Maryland, USA) (*right panel*). The results are the mean ± SEM ($n = 3$, $^{*}p < 0.05$). (B) *NCAM* expression levels in the TAM_Ls were determined by quantitative RT-PCR, compared with those of the Macrophage_Ls, and normalized to *GAPDH* expression. The results are the mean ± SEM ($n = 3$, $^{*}p < 0.05$). (C) NCAM induction was also confirmed in the TAM_Ls by western blotting (*left panel*). The results were normalized to β-actin as a control, and densitometric analysis of bands was performed with the ImageJ (*right panel*). The results are the mean ± SEM ($n = 3$, $^{*}p < 0.05$). (D) NCAM and CD11b expression in Macrophage_Ls and TAM_Ls. Double immunofluorescence was performed using anti-NCAM (green) plus the macrophage marker anti-CD11b (red). NCAM expression was detectable in TAM_Ls_TE-9 (*left panel*). Nuclei were stained with DAPI (blue). Scale bar, 10 μm. NCAM fluorescent intensity data were quantified using ImageJ (*right panel*). The corrected total cell fluorescence (CTCE) was calculated as integrated density – (area of selected cell × mean fluorescence of background reading). The results are the mean ± SEM ($n = 3$, $^{**}p < 0.001$). (E) The localization of NCAM and F-actin in TAM_Ls_TE-9. Immunofluorescence was performed using anti-NCAM (green) in TAM_Ls_TE-9. Nuclei and F-actin were stained with DAPI (blue) and phalloidin (red), respectively. NCAM and F-actin were co-localized at a part of the lamellipodia (*arrowheads*). Scale bar, 10 μm. (For interpretation of the references to color in this figure legend, the reader is referred to the web version of this article.)

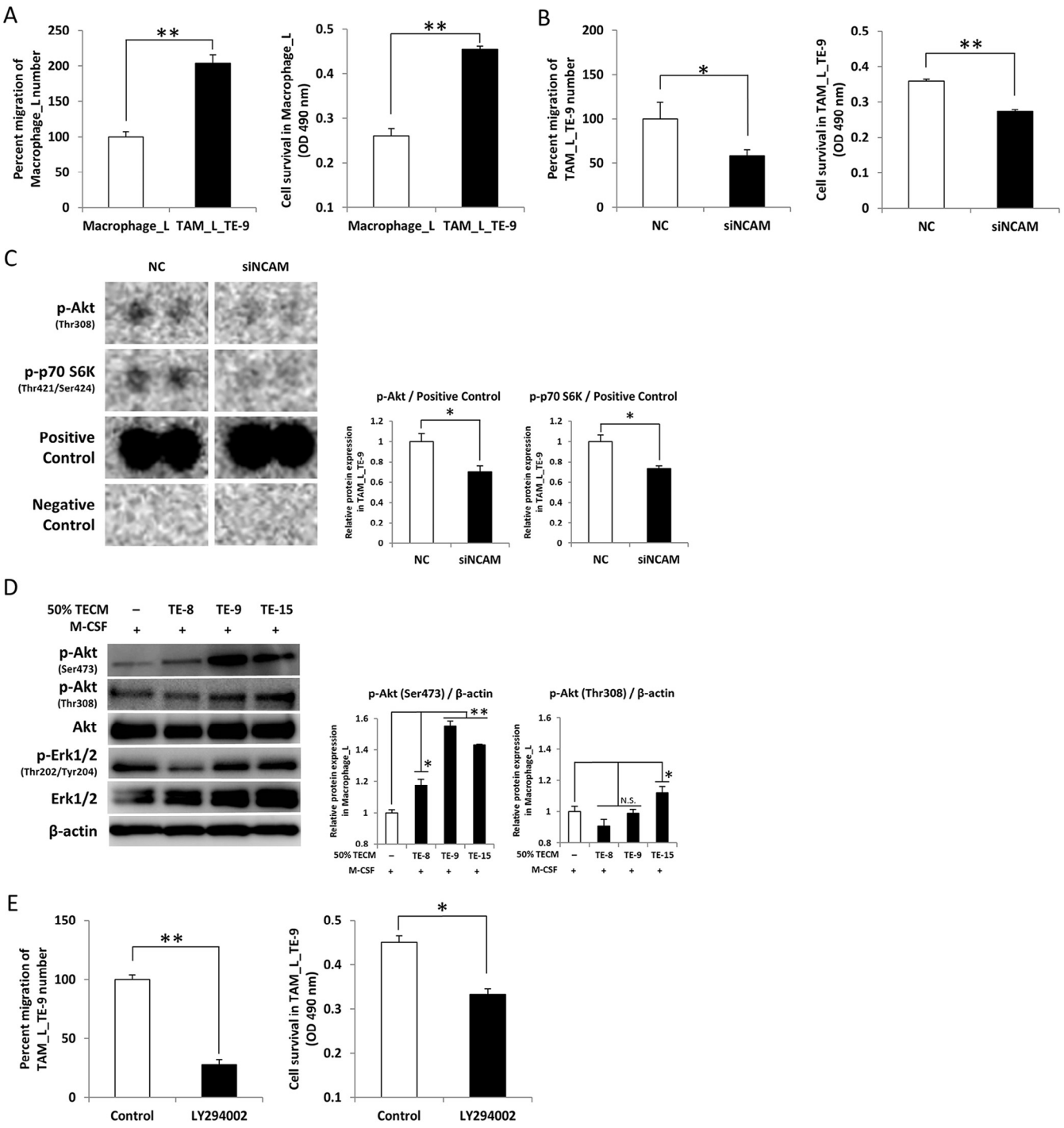

Fig. 2. The involvement of NCAM in the migration and survival of TAM_Ls via the activation of PI3K-Akt signaling. (A) The effect of TECM on Macrophage_Ls migration and survival. Transwell migration assay results (*left panel*): Macrophage_Ls and TAM_L_TE-9 were individually detached with Accutase and plated on Transwell cell culture inserts in DMEM supplemented with 1% human AB serum at a density of 1×10^5 cells/well. The cell inserts were set on 24-well plates in serum-free DMEM and then cultured for 24 h. The migrated cells on the underside of the membrane were stained with Diff-Quik and counted. Exposure to TE-9CM significantly promoted Macrophage_L migrations. The results are the mean ± SEM ($n = 3$, $^{**}p < 0.001$). Cell survival assay (*right panel*): Macrophage_Ls and TAM_Ls_TE-9 were individually detached with Accutase and seeded on 96-well plates at a density of 1×10^4 cells/well. The cell plates were cultured for 24 h in serum-free DMEM. Cell survival activity was assessed by MTS assay. Exposure to TE-9CM significantly promoted Macrophage_L cell survival. The results are the mean ± SEM ($n = 3$, $^{*}p < 0.05$, $^{**}p < 0.001$). (B) Knockdown of NCAM suppressed TAM_L migration and survival. Macrophage_Ls were transfected with siRNA for *NCAM* (siNCAM) or negative control (NC) for 6 h and then exposed to TE-9CM for 2 d to induce TAM_Ls_TE-9. Each of these detached cells was subjected to a migration assay and cell survival assay as in (A). The silencing of NCAM significantly reduced the migration (*left panel*) and survival of TAM_Ls_TE-9 (*right panel*). The results are the mean ± SEM (n = 3, $^{*}p < 0.05$). (C) The silencing of NCAM suppressed PI3K-Akt signaling in TAM_Ls_TE-9. Macrophage_Ls were transfected with 20 nM of *NCAM* siRNA (siNCAM) or negative control siRNA (NC) for 6 h and exposed to TE-9CM for 2 d to induce TAM_Ls_TE-9. The cells were cultured in serum-free DMEM for 24 h. The cell lysates were collected and applied to a Profiler Human Phosphokinase Array. The silencing of NCAM suppressed PI3K-Akt and p70 S6K (*left panel*). The results were normalized to a positive control, and densitometric analysis of bands was performed with the ImageJ (*middle and right panels*). The results are the mean ± SEM ($n = 3$, $^{*}p < 0.05$). (D) The effect of TECM on the PI3K-Akt signaling in Macrophage_Ls. The involvement of PI3K/Akt and Erk1/2 signaling between the Macrophage_Ls and TAM_Ls was assessed by western blotting. Phosphorylation of PI3K-Akt by TECM (TE-9 and TE-15) was detected (*left panel*). Erk1/2 phosphorylation did not appear to be stimulated by TECM (TE-8, TE-9 and TE-15). The results were normalized to β-actin as a control and densitometric analysis of bands was performed with the ImageJ (*middle and right panels*). The results are the mean ± SEM ($n = 3$, $^{*}p < 0.05$). (E) The effect of a selective PI3K inhibitor on the migration and survival of TAM_Ls. Detached TAM_Ls_TE-9 was pretreated with or without the selective PI3K inhibitor LY294002 (20 μM) for 24 h and then subjected to a migration assay and cell survival assay as in (A). TAM_Ls_TE-9 migration (*left panel*) and survival (*right panel*) were significantly inhibited by LY294002. The results are the mean ± SEM ($n = 3$, $^{*}p < 0.05$, $^{**}p < 0.001$).

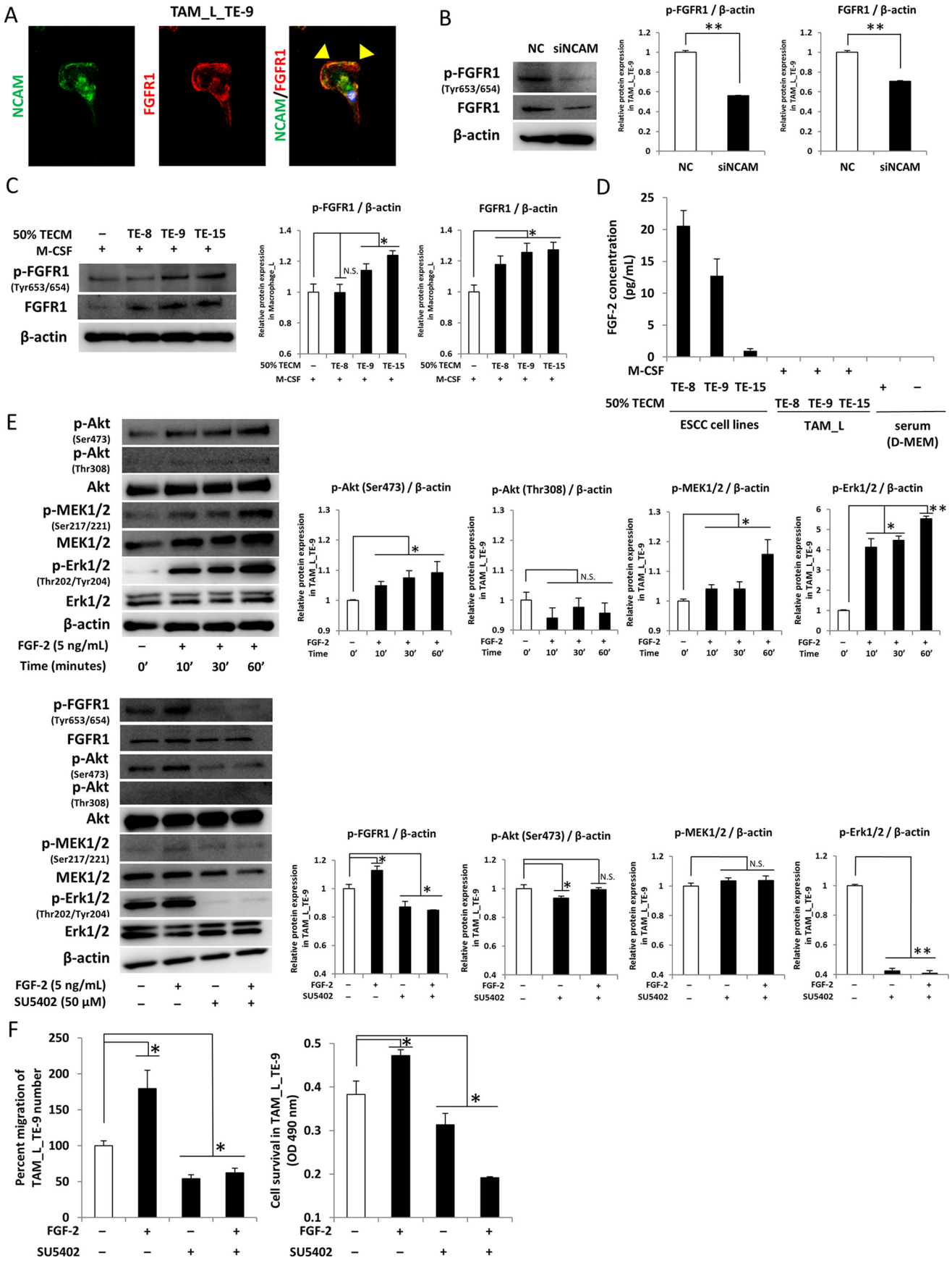
A
TAM_L_TE-9
NCAM
FGFR1
NCAM/FGFR1
B
NC siNCAM
p-FGFR1 (Tyr653/654)
FGFR1
β-actin
p-FGFR1 / β-actin
FGFR1 / β-actin
Relative protein expression in TAM_L_TE-9
NC
siNCAM
C
50% TECM – TE-8 TE-9 TE-15
M-CSF + + + +
p-FGFR1 (Tyr653/654)
FGFR1
β-actin
p-FGFR1 / β-actin
FGFR1 / β-actin
Relative protein expression in Macrophage_L
N.S.
D
FGF-2 concentration (pg/mL)
M-CSF
TE-8 TE-9 TE-15
50% TECM
ESCC cell lines
TAM_L
serum (D-MEM)
E
p-Akt (Ser473)
p-Akt (Thr308)
Akt
p-MEK1/2 (Ser217/221)
MEK1/2
p-Erk1/2 (Thr202/Tyr204)
Erk1/2
β-actin
FGF-2 (5 ng/mL)
Time (minutes) 0′ 10′ 30′ 60′
p-Akt (Ser473) / β-actin
p-Akt (Thr308) / β-actin
p-MEK1/2 / β-actin
p-Erk1/2 / β-actin
Relative protein expression in TAM_L_TE-9
FGF-2
Time
SU5402 (50 μM)
p-FGFR1 / β-actin
p-Akt (Ser473) / β-actin
p-MEK1/2 / β-actin
p-Erk1/2 / β-actin
SU5402
F
Percent migration of TAM_L_TE-9 number
Cell survival in TAM_L_TE-9 (OD 490 nm)
FGF-2
SU5402

Fig. 3. The NCAM/FGFR1 interaction induced a specific cellular response that was remarkably elicited by FGF-2 in TAM_Ls. (A) Co-expression of NCAM and FGFR1 in TAM_Ls. The double immunofluorescence examination of TAM_Ls_TE-9 was performed using anti-NCAM (green) and anti-FGFR1 (red) antibodies. NCAM and FGFR1 expression was co-localized mainly at the cell membranes of TAM_Ls_TE-9 (*arrowheads*). Scale bar, 10 μm. (B) The silencing of NCAM suppressed FGFR1 expression and phosphorylation in TAM_Ls. siNCAM or NC transfected with TAM_Ls_TE-9 was cultured for 24 h in serum-free DMEM. The cell lysates were collected, and each sample was analyzed by western blotting. NCAM silencing also suppressed FGFR1 expression and phosphorylation in TAM_Ls_TE-9 (*left panel*). The results were normalized to β-actin as a control, and densitometric analysis of bands was performed with ImageJ (*middle and right panels*). The results are the mean ± SEM ($n = 3$, $^{**}p < 0.001$). (C) FGFR1 expression in Macrophage_Ls and TAM_Ls. Western blotting showed that FGFR1 expression and phosphorylation were up-regulated in TAM_Ls (*left panel*). The results were normalized to β-actin as a control, and densitometric analysis of bands was performed with ImageJ (*middle and right panels*). The results are the mean ± SEM ($n = 3$, $^{*}p < 0.05$). (D) The concentration of FGF-2 protein in the conditioned medium of ESCC cell lines and TAM_Ls. Protein levels were measured by ELISA. The secreted FGF-2 levels in TE-8, TE-9 and TE-15 were 20.58 ± 2.38 pg/mL, 12.74 ± 2.67 pg/mL and 0.98 ± 0.35 pg/mL, respectively. In contrast, the FGF-2 secreted by TAM_Ls was undetectable. The data are the mean ± SEM in triplicate. (E) PI3K-Akt and MEK1/2-Erk1/2 phosphorylation in TAM_Ls by FGF-2. TAM_Ls_TE-9 was cultured for 24 h in serum-free DMEM in the presence or absence of recombinant protein (rhFGF-2, 5 ng/mL) and/or selective FGFR1 inhibitor (SU5402, 50 μM). Cells were pretreated with SU5402 1 h before adding rhFGF-2. FGF-2 treatment activated PI3K-Akt and MEK1/2-Erk1/2 signaling, and a persistent phosphorylation level was maintained up to 1 h in TAM_Ls_TE-9 (*upper left panel*). TAM_Ls_TE-9 was pretreated with SU5402 or untreated for 1 h followed by stimulation with rhFGF-2 for 1 h. rhFGF-2 significantly phosphorylated FGFR1, and pretreatment with SU5402 significantly inhibited FGFR1, Akt and Erk1/2 phosphorylation (*lower left panel*). The results were normalized to β-actin as a control, and densitometric analysis of bands was performed with ImageJ (*right panels*). The results are the mean ± SEM ($n = 3$, $^{*}p < 0.05$, $^{**}p < 0.001$). (F) Effect of FGF-2 on TAM_L migration and survivals. Transwell migration assay (*left panel*): TAM_Ls_TE-9 was detached with Accutase and plated on Transwell cell culture inserts at a density of 1×10^5 cells/well with DMEM supplemented with 1% human AB serum in the presence or absence of rhFGF-2 (5 ng/mL) and/or SU5402 (50 μM). Cells were pretreated with SU5402 for 1 h before adding rhFGF-2. The cells were placed on 24-well plate inserts in serum-free DMEM and then cultured for 24 h. The migrated cells on the underside of the membrane were stained with Diff-Quik and counted. The migration of TAM_Ls_TE-9 was significantly promoted by rhFGF-2. FGF-2-induced TAM_Ls_TE-9 migration was significantly inhibited by SU5402, and pretreatment with SU5402 was not responsive to rhFGF-2. The results are the mean ± SEM ($n = 3$, $^{*}p < 0.05$). Cell survival assay (*right panel*): TAM_Ls_TE-9 was detached with Accutase and seeded on 96-well plates at a density of 1×10^4 cells/well. The cell plates were cultured for 24 h in serum-free DMEM in the presence or absence of rhFGF-2 (5 ng/mL) and/or SU5402 (50 μM). Cells were pretreated with SU5402 for 1 h before adding rhFGF-2. Cell survival activity was assessed by MTS assay. The survival of TAM_Ls_TE-9 was significantly promoted by rhFGF-2. FGF-2-induced survival of TAM_Ls_TE-9 was significantly inhibited by SU5402, and pretreatment with SU5402 was not responsive to rhFGF-2. The results are presented as the mean ± SEM ($n = 3$, $^{*}p < 0.05$). (For interpretation of the references to color in this figure legend, the reader is referred to the web version of this article.)

Table 1
Expression levels of FGF-2 in ESCC environment and their association with clinicopathological parameters and infiltrating macrophage phenotypes.

	Number of cases	Expression of FGF-2[a]								
		Stroma		*p*-value	Nest		*p* value	Stroma and nest	Stroma and/or nest	*p*-value
		Low ($n = 35$)	High ($n = 35$)		Low ($n = 42$)	High ($n = 28$)		Low ($n = 21$)	High ($n = 49$)	
Age										
<65	33	17	16	N.S.	20	13	N.S.	11	22	N.S.
≥65	37	18	19		22	15		10	27	
Histological grade[b]										
HGIEN + WDSCC	16	11	5	N.S.	8	8	N.S.	5	11	N.S.
MDSCC + PDSCC	54	24	30		34	20		16	38	
Depth of tumor invasion[b]										
T1	49	31	18	0.001**	29	20	N.S.	20	29	0.003**
T2 + T3	21	4	17		13	8		1	20	
Lymphatic vessel invasion[b]										
Negative	37	22	15	N.S.	20	17	N.S.	14	23	N.S.
Positive	33	13	20		17	11		7	26	
Blood vessel invasion[b]										
Negative	43	28	15	0.001**	27	16	N.S.	18	25	0.006**
Positive	27	7	20		15	12		3	24	
Lymph node metastasis[b]										
Negative	43	16	17	N.S.	15	18	N.S.	16	17	0.001**
Positive	27	19	18		27	10		5	32	
Stage[c]										
0 + I	38	25	13	0.004**	22	16	N.S.	16	22	0.016*
II + III + IV	32	10	22		20	12		5	27	
CD68 positive cells[d]										
Low	35	21	14	N.S.	17	18	N.S.	12	23	N.S.
High	35	14	21		25	10		9	26	
CD163 positive cells[d]										
Low	35	23	12	0.009**	18	17	N.S.	13	22	N.S.
High	35	12	23		24	11		8	27	
CD204 positive cells[d]										
Low	34	26	8	<0.0001***	17	17	N.S.	15	19	0.012*
High	36	9	27		25	11		6	30	

Data were analyzed by χ^2-test. $p < 0.05$ was considered statistically significant: $^{*}p < 0.05$; $^{**}p < 0.01$; $^{***}p < 0.001$.

[a] The site of localization of FGF-2 expression was divided into three parts as follows: cancer stroma, cancer nests and both cancer nests and stroma. These three parts were further categorized as low- and high-intensity groups.

[b] According to the Japanese Classification of Esophageal Cancer [26]. HGIEN, high-grade intraepithelial neoplasia; WDSCC, well-differentiated squamous cell carcinoma; MDSCC, moderately differentiated squamous cell carcinoma; PDSCC, poorly differentiated squamous cell carcinoma. T1a, tumor invades mucosa; T1b, tumor invades submucosa; T2, tumor invades muscularis propria; T3, tumor invades adventitia.

[c] According to the TNM classification by UICC [27].

[d] The median values of CD68 positive, CD163 positive or CD204 positive macrophage numbers in cancer nests and stroma within the areas were used to divide the patients into low- and high-groups.

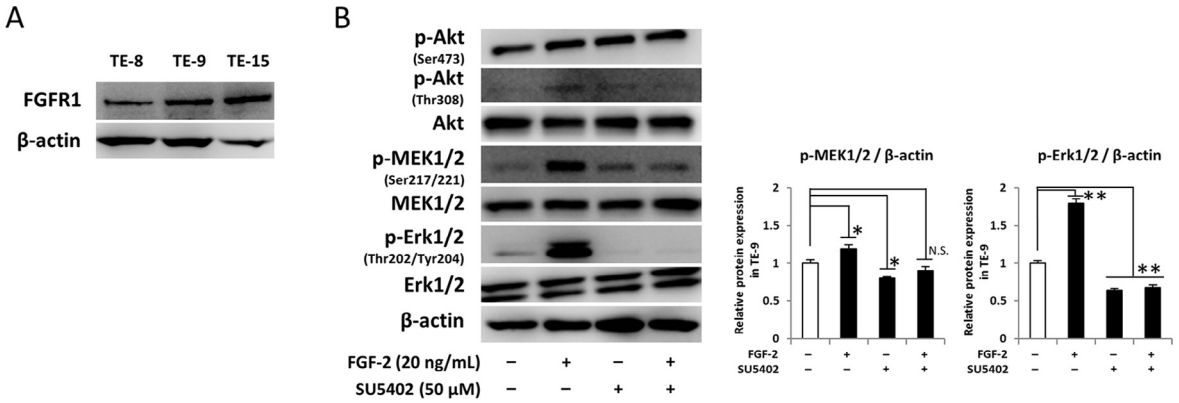
A
TE-8
TE-9
TE-15
FGFR1
β-actin
B
p-Akt (Ser473)
p-Akt (Thr308)
Akt
p-MEK1/2 (Ser217/221)
MEK1/2
p-Erk1/2 (Thr202/Tyr204)
Erk1/2
β-actin
FGF-2 (20 ng/mL)
SU5402 (50 μM)
p-MEK1/2 / β-actin
p-Erk1/2 / β-actin
Relative protein expression in TE-9
N.S.

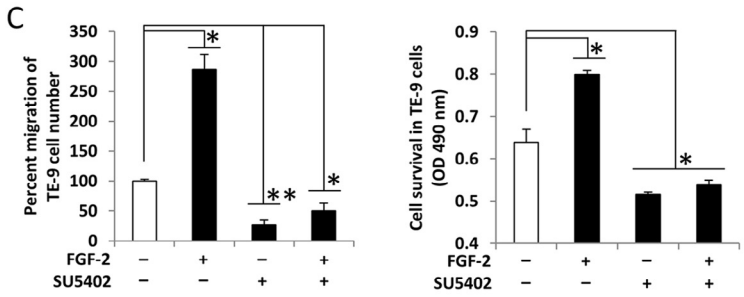
C
Percent migration of TE-9 cell number
Cell survival in TE-9 cells (OD 490 nm)
FGF-2
SU5402

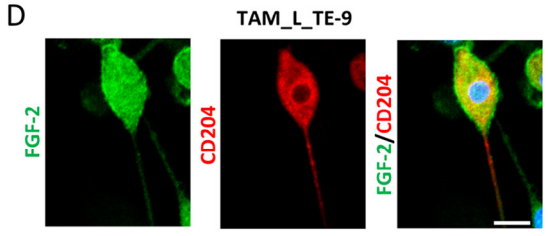
D
TAM_L_TE-9
FGF-2
CD204
FGF-2/CD204

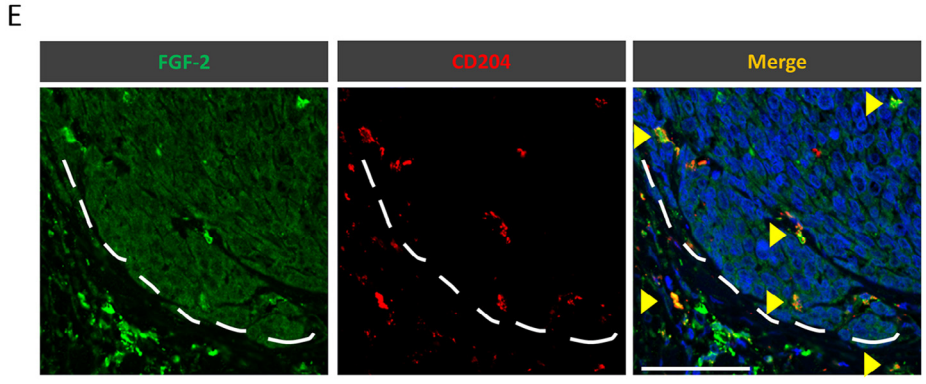
E
FGF-2
CD204
Merge

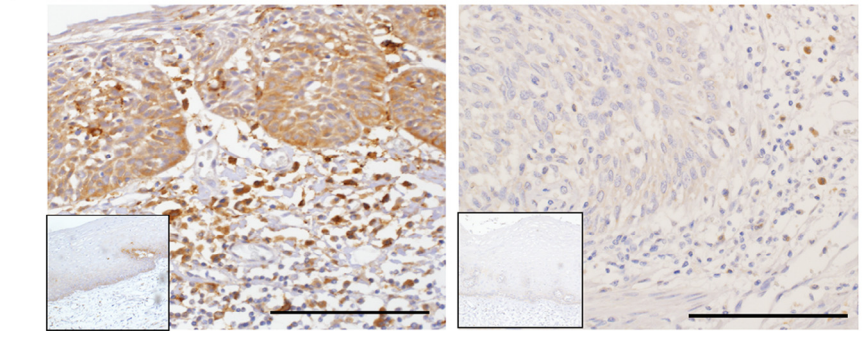
F

Fig. 4. High FGF-2 expression was detected not only in cancer cells but also their surrounding stromal cells of human ESCC tissues, and this expression may activate the FGF-2/FGFR1 loop for cancer cell migration and survival. (A) FGFR1 expression in the ESCC cell lines. FGFR1 expression levels were detected in all three ESCC cell lines (TE-8, TE-9 and TE-15) by western blotting. (B) The effect of FGF-2 on MEK1/2-Erk1/2 signaling in the ESCC cell lines. Western blotting (*left panel*): TE-9 cells were cultured for 24 h with serum-free DMEM in the presence or absence of rhFGF-2 (20 ng/mL) for 1 h and/or SU5402 (50 μM). Cells were pretreated with SU5402 for 1 h before adding rhFGF-2. rhFGF-2 treatment activated MEK1/2-Erk1/2 in TE-9. Pretreatment with SU5402 suppressed MEK1/2-Erk1/2 signaling in TE-9 cells. PI3K-Akt phosphorylation did not appear to be stimulated by rhFGF-2 and SU5402 in TE-9. The results were normalized to β-actin as a control and densitometric analysis of bands was performed with ImageJ (*middle and right panels*). The results are the mean ± SEM ($n = 3$, $^{**}p < 0.001$). (C) FGF-2 promoted ESCC cell survival and migration. The ESCC cell lines were detached with trypsin-EDTA. The Transwell migration assay (*left panel*) and cell survival assay (*right panel*) also followed the same process as that described in Fig. 3F. TE-9 survival was significantly promoted by rhFGF-2 (20 ng/mL). The FGF-2-induced migration and survival of TE-9 were significantly inhibited by SU5402 (50 μM), and pretreatment with SU5402 did not affect the stimulation of FGF-2. The results are the mean ± SEM ($n = 3$, $^{*}p < 0.05$, $^{**}p < 0.001$). (D) FGF-2 expression in Macrophage_Ls and TAM_Ls. A double immunofluorescence analysis of TAM_Ls_TE-9 was performed using anti-FGF-2 antibody (green) and the M2 macrophage marker anti-CD204 (red) antibody. FGF-2 and CD204 co-expression was detectable in TAM_Ls_TE-9. TAM_Ls_TE-9 expressing FGF-2 also expressed CD204. Nuclei were stained with DAPI (blue). Scale bar, 10 μm. (E) Cancer cells and cancer stromal cells, including $CD204^{+}$ TAMs, expressed FGF-2 in human ESCC tissues. Double immunofluorescence was performed using anti-FGF-2 (green) and anti-CD204 (red) antibodies in human ESCC tissue. FGF-2 was expressed in both cancer nests and cancer stroma, and some of the FGF-2 positive cells were $CD204^{+}$ macrophages. *Arrowheads* indicate FGF-2- and CD204-positive macrophages in both the cancer nests and stroma of the human ESCC tissue. Nuclei were stained with DAPI (blue). Scale bar, 50 μm. (F) Representative FGF-2 immunoreactivity of cancer nests and their surrounding stroma in human ESCC tissues. Typical images of FGF-2 high-intensity (*left panel*) and FGF-2 low-intensity (*right panel*) immunoreactivity in the ESCC tissues. In the tissue with high-intensity FGF-2, both cancer nests and their surrounding stroma exhibited increased cytoplasmic FGF-2 immunoreactivity compared with the corresponding nonneoplastic squamous epithelium (*insets*). The intensity of FGF-2 immunoreactivity was equal to that of the corresponding nonneoplastic squamous epithelium (*insets*) in the FGF-2 low-intensity cancer tissue. Scale bar, 50 μm. (For interpretation of the references to color in this figure legend, the reader is referred to the web version of this article.)

NCAM in TAM_Ls was morphologically co-localized with NCAM and a part of the lamellipodia that is involved in chemotaxis. Another study showed that stimulation with M-CSF led to lamellipodia formation in macrophages and induced migration and chemotaxis [34]. In adenoid cystic carcinoma cells grown on laminin, NCAM expression was selectively distributed to the lamellipodia, suggesting its participation in cell migration [35].

Roles of NCAM in intracellular signaling have been reported in various cell types [36,37]. Shi et al. indicated that NCAM potentiated cellular invasion and metastasis by activating PKA-PI3K signaling in melanoma cells [22]. NCAM is also a non-canonical ligand for FGFR1. NCAM binding is involved in sustained activation and recycling by preventing FGFR1 ubiquitination and degradation [30]. Moreover, a previous study reported that the activation of NCAM-mediated FGFR1 downstream signaling factors, such as PI3K-Akt and Erk1/2, is involved in neurite outgrowth and tumor progression [38–40]. In the present study, the NCAM expression induced TAM_L migration and survival through PI3K-Akt signaling. NCAM expression was involved in the retention of the expression level of FGFR1 and its phosphorylation in TAM_Ls. These findings suggest novel roles of NCAM in TAMs.

The acquisition of the M2-like phenotype is involved in chemotaxis and macrophage survival [41,42]. A recent study demonstrated that the M2 polarization of macrophages in the gastric cancer microenvironment promoted their chemotaxis and survival through the activation of Akt, Erk1/2 and STAT3 signaling [43]. In the present study, TECM exposure induced the migration and survival of Macrophage_Ls through PI3K-Akt signaling. In addition, TECM stimulation up-regulated the expression levels of FGFR1 and its phosphorylation in Macrophage_Ls. These results indicated that macrophages acquired M2-like characters via the up-regulation of NCAM and FGFR1, resulting in TAM migration and survival within the tumor microenvironment of ESCC.

A recent study reported that inhibition of FGF-2-mediated FGFR signaling could offer a better treatment option for patients with advanced, relapsed or refractory cancers [44]. FGF-2 is a member of the FGF family that is expressed in various normal cells. Macrophages also express and secrete FGF-2 [45,46]. FGF-2 occurs in four isoforms. The low-molecular-weight isoform (LMW FGF-2, 18 kDa) exhibits characteristic autocrine, paracrine and intracrine effects [47]. FGF-2 promotes the chemotaxis and proliferation of endothelial cells through Erk1/2 signaling, resulting in wound repair [48,49]. The autocrine, paracrine and intracrine growth promotion of FGF-2/FGFR1 signaling has been confirmed in various tumors [50–53]. In macrophages, the induction of vasculogenic mimicry formation in multiple myeloma is involved in the promotion of macrophage chemotaxis through an FGF-2/FGFR1 paracrine mechanism [54].

In the present study, FGF-2 stimulation induced the migration and survival of TECM-induced Macrophage_Ls and TE cells. PI3K-Akt and MEK1/2-Erk1/2 signaling were activated in TAM_Ls by FGF-2, and MEK1/2-Erk1/2 signaling was activated in TE cells by FGF-2. Chernykh et al. reported that FGF-2 was secreted by macrophages [46], but our present investigation was not able to confirm the secretion of FGF-2. However, our *in vitro* (Fig. 4D) and *in vivo* (Fig. 4E) experiments demonstrated FGF-2 protein expression in TAMs. In addition, FGF-2 exerts cellular activities through nuclear FGF-2/FGF1 intracrine mechanisms in pancreatic stellate cells [53]. We also confirmed the expression of FGF-2 and FGFR1 in the cytoplasm and nuclei of TAM_L_TE-9. These data may indicate that FGF-2 promotes the migration and survival of TAM_Ls and ESCC cells though FGFR1 signaling.

A recent study reported that FGFR1 activating factors, such as NCAM-derived- and FGF-2-agonists, could offer better therapeutic targets of neurodegenerative disorders [55]. However, the association between NCAM-induced FGFR1 and FGF-2-induced FGFR1 signaling remains elusive. The F3 module 2 structure of NCAM binds to FGFR directly, and FGF-2 coordinates the FGFR signal by having a structure similar to that F3 module 2 of NCAM [56,57]. Ditlevsen et al. also demonstrated that NCAM- and FGF-2-mediated FGFR1 signaling shares many common pathways, such as Akt and Erk1/2 [58]. The dramatic divergence between NCAM- and FGF-2-mediated FGFR1 signaling can be explained by the intracellular trafficking of FGFR1. FGF-2-mediated FGFR1 signaling induces the classical route of Cbl-mediated ubiquitination followed by lysosomal degradation, whereas NCAM-mediated FGFR1 signaling promotes FGFR1 stabilization and recycling [30,59]. In addition, Francavilla et al. reported that NCAM and FGF-2 bind to a different tyrosine residue in FGFR and cause specific respective responses [30]. In the present study, both NCAM- and FGF-2-mediated FGFR1 signaling phosphorylated Tyr653/654, which is essential for activation of FGFR1 tyrosine kinase activity [60].

Previous studies showed that up-regulated FGF-2 correlated with a poor prognosis in pancreatic ductal carcinoma and glioma [61,62] but not in breast cancer [63]. In the present study, we analyzed the relationship between FGF-2 expression and clinicopathological parameters in cancer nests and stroma separately because some of the FGF-2-positive stromal cells expressed CD204 in ESCC. Similar to the previous report [33], our prognostic analysis showed no prognostic significance of the up-regulation of FGF-2 in cancer nests or stroma. In addition to a clinicopathological correlation, our findings

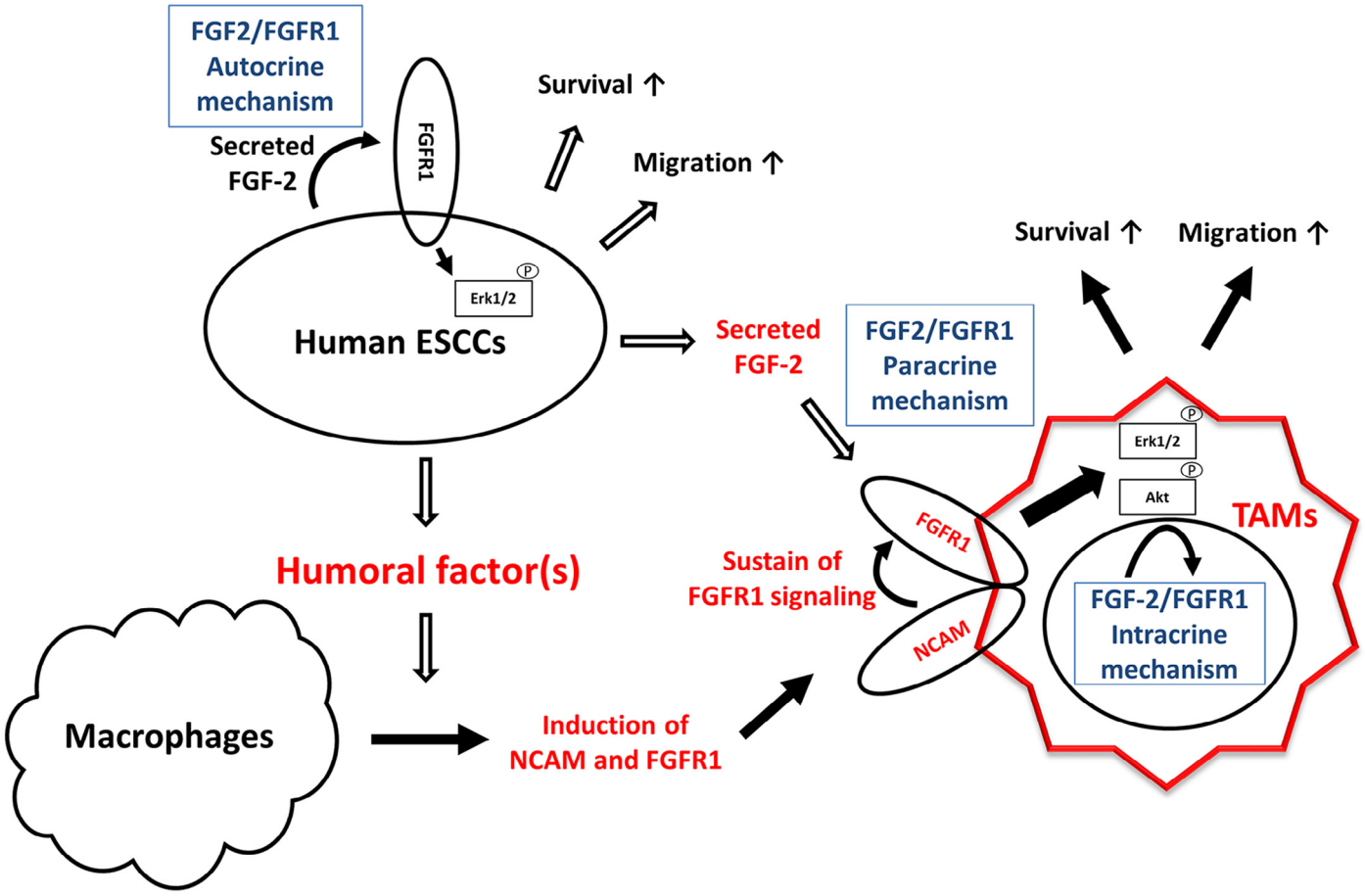

Fig. 5. A proposed model of the interplay between NCAM/FGFR1 and FGF-2/FGFR1 in the tumor microenvironment of ESCCs. NCAM up-regulation in the macrophages was induced by various humoral factors of ESCCs. The up-regulated NCAM is involved in migration and survival of TAMs through PI3K-Akt and FGFR1 signaling. The secreted FGF-2 from tumor cells promotes migration and survival of TAMs and itself through an FGF-2/FGFR1 loop. FGF-2 expression in TAMs also activates the FGF-2/FGFR1 intracrine loop.

revealed for the first time an association between up-regulated FGF-2 within cancer stroma and infiltrated M2 macrophages. These data imply that the up-regulation of FGF-2 in stromal cells, including TAMs, promoted tumor formation through an FGF-2/FGFR1 intracrine and paracrine loop in TAMs.

In summary, NCAM expression may play roles not only in FGFR1 expression levels but also in the regulation of FGF-2/FGFR1 intracrine and paracrine mechanisms in TAMs (Fig. 5). These findings indicate a novel role of NCAM- and FGF-2-mediated FGFR1 signaling in ESCCs, including TAMs. Our results suggest that these molecules could become new biomarkers and could be used in cancer therapy targeted against the progression of ESCC.

Authors' contributions

NT, YK, NA and HA conceived and performed the experiments. YK and HY analyzed the data and wrote the manuscript. NU, MN and MS prepared the tissue samples and performed the histological classification.

Acknowledgements

This work was supported by Grants-in-Aid for Scientific Research (C-23590397) and (C-26460418) and for Young Scientists (B-26870364) from the Japan Society for the Promotion of Science. We thank Dr. Shuho Semba for the valuable discussions and technical suggestions. We thank Atsuko Kawashima, Yumi Hashimoto, Nobuo Kubo, Miki Yamazaki and Shuichi Matsumoto for their excellent technical assistance.

Conflict of interest

None to declare.

Appendix: Supplementary material

Supplementary data to this article can be found online at doi:10.1016/j.canlet.2016.06.009.

References

[1] F. Balkwill, K.A. Charles, A. Mantovani, Smoldering and polarized inflammation in the initiation and promotion of malignant disease, Cancer Cell 7 (2005) 211–217.
[2] A. Mantovani, S. Sozzani, M. Locati, P. Allavena, A. Sica, Macrophage polarization: tumor-associated macrophages as a paradigm for polarized M2 mononuclear phagocytes, Trends Immunol. 23 (2002) 549–555.
[3] T. Chanmee, P. Ontong, K. Konno, N. Itano, Tumor-associated macrophages as major players in the tumor microenvironment, Cancers (Basel) 6 (2014) 1670–1690.
[4] A. Mantovani, T. Schioppa, C. Porta, P. Allavena, A. Sica, Role of tumor-associated macrophages in tumor progression and invasion, Cancer Metastasis Rev. 25 (2006) 315–322.
[5] M. Heusinkveld, S.H. van der Burg, Identification and manipulation of tumor associated macrophages in human cancers, J. Transl. Med. 9 (2011) 216.
[6] B.Z. Qian, J.W. Pollard, Macrophage diversity enhances tumor progression and metastasis, Cell 141 (2010) 39–51.

[7] Y. Komohara, D. Niino, Y. Saito, K. Ohnishi, H. Horlad, K. Ohshima, et al., Clinical significance of CD163(+) tumor-associated macrophages in patients with adult T-cell leukemia/lymphoma, Cancer Sci. 104 (2013) 945–951.

[8] L. Yang, F. Wang, L. Wang, L. Huang, J. Wang, B. Zhang, et al., CD163+ tumor-associated macrophage is a prognostic biomarker and is associated with therapeutic effect on malignant pleural effusion of lung cancer patients, Oncotarget 6 (2015) 10592–10603.

[9] Y. Komohara, K. Ohnishi, J. Kuratsu, M. Takeya, Possible involvement of the M2 anti-inflammatory macrophage phenotype in growth of human gliomas, J. Pathol. 216 (2008) 15–24.

[10] M. Shigeoka, N. Urakawa, T. Nakamura, M. Nishio, T. Watajima, D. Kuroda, et al., Tumor associated macrophage expressing CD204 is associated with tumor aggressiveness of esophageal squamous cell carcinoma, Cancer Sci. 104 (2013) 1112–1119.

[11] C.N. Lin, C.J. Wang, Y.J. Chao, M.D. Lai, Y.S. Shan, The significance of the co-existence of osteopontin and tumor-associated macrophages in gastric cancer progression, BMC Cancer 15 (2015) 128.

[12] E.A. Montgomery, F.T. Bosman, P. Brennan, R. Malekzadeh, Oesophageal cancer, in: B.W. Stewart, C.P. Wild (Eds.), World Cancer Report 2014, IARC, Lyon, 2014, pp. 374–382.

[13] A. Pennathur, M.K. Gibson, B.A. Jobe, J.D. Luketich, Oesophageal carcinoma, Lancet 381 (2013) 400–412.

[14] M.K. Gibson, Up To Date: epidemiology, pathobiology, and clinical manifestations of esophageal cancer. <http://www.uptodate.com/contents/epidemiology-pathobiology-and-clinical-manifestations-of-esophageal-cancer>, (accessed 26.08.15).

[15] N. Urakawa, S. Utsunomiya, M. Nishio, M. Shigeoka, N. Takase, N. Arai, et al., GDF15 derived from both tumor-associated macrophages and esophageal squamous cell carcinomas contributes to tumor progression via Akt and Erk pathways, Lab. Invest. 95 (2015) 491–503.

[16] M. Shigeoka, N. Urakawa, M. Nishio, N. Takase, S. Utsunomiya, H. Akiyama, et al., Cyr61 promotes CD204 expression and the migration of macrophages via MEK/ERK pathway in esophageal squamous cell carcinoma, Cancer Med. 4 (2015) 437–446.

[17] U. Rutishauser, J.P. Thiery, R. Brackenbury, B.A. Sela, G.M. Edelman, Mechanisms of adhesion among cells from neural tissues of the chick embryo, Proc. Natl. Acad. Sci. U.S.A. 73 (1976) 577–581.

[18] R. Bertolotti, U. Rutishauser, G.M. Edelman, A cell surface molecule involved in aggregation of embryonic liver cells, Proc. Natl. Acad. Sci. U.S.A. 77 (1980) 4831–4835.

[19] B.A. Cunningham, S. Hoffman, U. Rutishauser, J.J. Hemperly, G.M. Edelman, Molecular topography of the neural cell adhesion molecule N-CAM: surface orientation and location of sialic acid-rich and binding regions, Proc. Natl. Acad. Sci. U.S.A. 80 (1983) 3116–3120.

[20] L.C. Ronn, V. Berezin, E. Bock, The neural cell adhesion molecule in synaptic plasticity and ageing, Int. J. Dev. Neurosci. 18 (2000) 193–199.

[21] G. Sconocchia, K. Keyvanfar, F. El Ouriaghli, M. Grube, K. Rezvani, H. Fujiwara, et al., Phenotype and function of a CD56+ peripheral blood monocyte, Leukemia 19 (2005) 69–76.

[22] Y. Shi, R. Liu, S. Zhang, Y.Y. Xia, H.J. Yang, K. Guo, et al., Neural cell adhesion molecule potentiates invasion and metastasis of melanoma cells through CAMP-dependent protein kinase and phosphatidylinositol 3-kinase pathways, Int. J. Biochem. Cell Biol. 43 (2011) 682–690.

[23] P.B. Campodonico, E.D. de Kier Joffe, A.J. Urtreger, L.S. Lauria, J.M. Lastiri, L.I. Puricelli, et al., The neural cell adhesion molecule is involved in the metastatic capacity in a murine model of lung cancer, Mol. Carcinog. 49 (2010) 386–397.

[24] S. Xu, X. Li, J. Zhang, J. Chen, Prognostic value of CD56 in patients with acute myeloid leukemia: a meta-analysis, J. Cancer Res. Clin. Oncol. 141 (2015) 1859–1870.

[25] Y. Pan, H. Wang, Q. Tao, C. Zhang, D. Yang, H. Qin, et al., Absence of both CD56 and CD117 expression on malignant plasma cell is related with a poor prognosis in patients with newly diagnosis multiple myeloma, Leuk. Res. 40 (2016) 77–82.

[26] Japan Esophageal Society, Japanese Classification of Esophageal Cancer, tenth ed., Kanehara & Co, Tokyo, 2008.

[27] L.H. Sobin, M.K. Gospodarowicz, C. Wittekind (eds), TNM Classification of Malignant Tumours, seventh ed., Wiley-Blackwell, Hoboken, NJ, 2011.

[28] L. Perey, J. Benhattar, R. Peters, P. Jaunin, S. Leyvraz, High tumour contamination of leukaphereses in patients with small cell carcinoma of the lung: a comparison of immunocytochemistry and RT-PCR, Br. J. Cancer 85 (2001) 1713–1721.

[29] H. Hasita, Y. Komohara, H. Okabe, T. Masuda, K. Ohnishi, X.F. Lei, et al., Significance of alternatively activated macrophages in patients with intrahepatic cholangiocarcinoma, Cancer Sci. 101 (2010) 1913–1919.

[30] C. Francavilla, P. Cattaneo, V. Berezin, E. Bock, D. Ami, A. de Marco, et al., The binding of NCAM to FGFR1 induces a specific cellular response mediated by receptor trafficking, J. Cell Biol. 187 (2009) 1101–1116.

[31] S.E. Hughes, Differential expression of the fibroblast growth factor receptor (FGFR) multigene family in normal human adult tissues, J. Histochem. Cytochem. 45 (1997) 1005–1019.

[32] C. Barclay, A.W. Li, L. Geldenhuys, M. Baguma-Nibasheka, G.A. Porter, P.J. Veugelers, et al., Basic fibroblast growth factor (FGF-2) overexpression is a risk factor for esophageal cancer recurrence and reduced survival, which is ameliorated by coexpression of the FGF-2 antisense gene, Clin. Cancer Res. 11 (2005) 7683–7691.

[33] K. Sugiura, S. Ozawa, Y. Kitagawa, M. Ueda, M. Kitajima, Co-expression of aFGF and FGFR-1 is predictive of a poor prognosis in patients with esophageal squamous cell carcinoma, Oncol. Rep. 17 (2007) 557–564.

[34] G.E. Jones, Cellular signaling in macrophage migration and chemotaxis, J. Leukoc. Biol. 68 (2000) 593–602.

[35] C.M. Franca, M.M. Jaeger, R.G. Jaeger, N.S. Araujo, The role of basement membrane proteins on the expression of neural cell adhesion molecule (N-CAM) in an adenoid cystic carcinoma cell line, Oral Oncol. 36 (2000) 248–252.

[36] Y. Shi, Y.Y. Xia, L. Wang, R. Liu, K.S. Khoo, Z.W. Feng, Neural cell adhesion molecule modulates mesenchymal stromal cell migration via activation of MAPK/ERK signaling, Exp. Cell Res. 318 (2012) 2257–2267.

[37] D.K. Ditlevsen, L.B. Kohler, M.V. Pedersen, M. Risell, K. Kolkova, M. Meyer, et al., The role of phosphatidylinositol 3-kinase in neural cell adhesion molecule-mediated neuronal differentiation and survival, J. Neurochem. 84 (2003) 546–556.

[38] D.K. Ditlevsen, G.K. Povlsen, V. Berezin, E. Bock, NCAM-induced intracellular signaling revisited, J. Neurosci. Res. 86 (2008) 727–743.

[39] R. Liu, Y. Shi, H.J. Yang, L. Wang, S. Zhang, Y.Y. Xia, et al., Neural cell adhesion molecule potentiates the growth of murine melanoma via beta-catenin signaling by association with fibroblast growth factor receptor and glycogen synthase kinase-3beta, J. Biol. Chem. 286 (2011) 26127–26137.

[40] S. Zecchini, L. Bombardelli, A. Decio, M. Bianchi, G. Mazzarol, F. Sanguineti, et al., The adhesion molecule NCAM promotes ovarian cancer progression via FGFR signalling, EMBO Mol. Med. 3 (2011) 480–494.

[41] G. Solinas, G. Germano, A. Mantovani, P. Allavena, Tumor-associated macrophages (TAM) as major players of the cancer-related inflammation, J. Leukoc. Biol. 86 (2009) 1065–1073.

[42] S.C. Huang, B. Everts, Y. Ivanova, D. O'Sullivan, M. Nascimento, A.M. Smith, et al., Cell-intrinsic lysosomal lipolysis is essential for alternative activation of macrophages, Nat. Immunol. 15 (2014) 846–855.

[43] T. Yamaguchi, S. Fushida, Y. Yamamoto, T. Tsukada, J. Kinoshita, K. Oyama, et al., Tumor-associated macrophages of the M2 phenotype contribute to progression in gastric cancer with peritoneal dissemination, Gastric Cancer (2015) doi:10.1007/s10120-015-0579-8.

[44] M.R. Aki, P. Nagpal, N.M. Ayoub, B. Tai, S.A. Prabhu, C.M. Capac, et al., Molecular and clinical significance of fibroblast growth factor 2 (FGF2/bFGF) in malignancies of solid and hematological cancers for personalized therapies, Oncotarget (2016) doi:10.18632/oncotarget.8203.

[45] C. Henke, W. Marineili, J. Jessurun, J. Fox, D. Harms, M. Peterson, et al., Macrophage production of basic fibroblast growth factor in the fibroproliferative disorder of alveolar fibrosis after lung injury, Am. J. Pathol. 143 (1993) 1189–1199.

[46] E.R. Chernykh, E.Y. Shevela, L.V. Sakhno, M.A. Tikhonova, Y.L. Petrovsky, A.A. Ostanin, The generation and properties of human M2-like macrophages: potential candidates for CNS repair?, Cell. Ther. Transplant. 2 (2010) doi:10.3205/ctt-2010-en-000080.01 e.000080.01.

[47] M. Arese, Y. Chen, R.Z. Florkiewicz, A. Gualandris, B. Shen, D.B. Rifkin, Nuclear activities of basic fibroblast growth factor: potentiation of low-serum growth mediated by natural or chimeric nuclear localization signals, Mol. Biol. Cell 10 (1999) 1429–1444.

[48] Z. Qu, M. Picou, T.T. Dang, E. Angell, S.R. Planck, C.E. Hart, et al., Immunolocalization of basic fibroblast growth factor and platelet-derived growth factor-A during adjuvant arthritis in the Lewis rat, Am. J. Pathol. 145 (1994) 1127–1139.

[49] G. Pintucci, D. Moscatelli, F. Saponara, P.R. Biernacki, F.G. Baumann, C. Bizekis, et al., Lack of ERK activation and cell migration in FGF-2-deficient endothelial cells, FASEB J. 16 (2002) 598–600.

[50] M. Kin, M. Sata, T. Ueno, T. Torimura, S. Inuzuka, R. Tsuji, et al., Basic fibroblast growth factor regulates proliferation and motility of human hepatoma cells by an autocrine mechanism, J. Hepatol. 27 (1997) 677–687.

[51] G. Lefevre, N. Babchia, A. Calipel, F. Mouriaux, A.M. Faussat, S. Mrzyk, et al., Activation of the FGF2/FGFR1 autocrine loop for cell proliferation and survival in uveal melanoma cells, Invest. Ophthalmol. Vis. Sci. 50 (2009) 1047–1057.

[52] J.K. Dow, R.W. deVere White, Fibroblast growth factor 2: its structure and property, paracrine function, tumor angiogenesis, and prostate-related mitogenic and oncogenic functions, Urology 55 (2000) 800–806.

[53] S.J. Coleman, A.M. Chioni, M. Ghallab, R.K. Anderson, N.R. Lemoine, H.M. Kocher, et al., Nuclear translocation of FGFR1 and FGF2 in pancreatic stellate cells facilitates pancreatic cancer cell invasion, EMBO Mol. Med. 6 (2014) 467–481.

[54] S. Berardi, R. Ria, A. Reale, A. De Luisi, I. Catacchio, M. Moschetta, et al., Multiple myeloma macrophages: pivotal players in the tumor microenvironment, J. Oncol. 2013 (2013) 183602.

[55] M.E. Woodbury, T. Ikezu, Fibroblast growth factor-2 signaling in neurogenesis and neurodegeneration, J. Neuroimmune Pharmacol. 9 (2014) 92–101.

[56] V.V. Kiselyov, G. Skladchikova, A.M. Hinsby, P.H. Jensen, N. Kulahin, V. Soroka, et al., Structural basis for a direct interaction between FGFR1 and NCAM and evidence for a regulatory role of ATP, Structure 11 (2003) 691–701.

[57] C.J. Powers, S.W. McLeskey, A. Wellstein, Fibroblast growth factors, their receptors and signaling, Endocr. Relat. Cancer 7 (2000) 165–197.

[58] D.K. Ditlevsen, S. Owczarek, V. Berezin, E. Bock, Relative role of upstream regulators of Akt, ERK and CREB in NCAM- and FGF2-mediated signalling, Neurochem. Int. 53 (2008) 137–147.

[59] A. Wong, B. Lamothe, A. Lee, J. Schlessinger, I. Lax, FRS2α attenuates FGF receptor signaling by Grb2-mediated recruitment of the ubiquitin ligase Cbl, Proc. Natl. Acad. Sci. U.S.A. 99 (2002) 6684–6689.

[60] M. Mohammadi, I. Dikic, A. Sorokin, W.H. Burgess, M. Jaye, J. Schlessinger, Identification of six novel autophosphorylation sites on fibroblat growth factor receptor 1 and elucidation of their importance in receptor activation and signal transduction, Mol. Cell. Biol. 16 (1996) 977–989.
[61] K. Kuwahara, T. Sasaki, Y. Kuwada, M. Murakami, S. Yamasaki, K. Chayama, Expressions of angiogenic factors in pancreatic ductal carcinoma: a correlative study with clinicopathologic parameters and patient survival, Pancreas 26 (2003) 344–349.
[62] L. Sooman, E. Freyhult, A. Jaiswal, S. Navani, P.H. Edqvist, F. Ponten, et al., FGF2 as a potential prognostic biomarker for proneural glioma patients, Acta Oncol. 54 (2015) 385–394.
[63] B.K. Linderholm, B. Lindh, L. Beckman, M. Erlanson, K. Edin, B. Travelin, et al., Prognostic correlation of basic fibroblast growth factor and vascular endothelial growth factor in 1307 primary breast cancers, Clin. Breast Cancer 4 (2003) 340–347.